



Available online at <http://scik.org>

Commun. Math. Biol. Neurosci. 2021, 2021:36

<https://doi.org/10.28919/cmbn/5590>

ISSN: 2052-2541

MATHEMATICAL ANALYSIS OF TYPHOID FEVER TRANSMISSION DYNAMICS WITH SEASONALITY AND FEAR

LUNGA MATSEBULA¹, FARAI NYABADZA^{1,*}, JOSIAH MUSHANYU²

¹Department of Mathematics and Applied Mathematics, University of Johannesburg, South Africa

²Department of Mathematics, University of Zimbabwe, Harare, Zimbabwe

Copyright © 2021 the author(s). This is an open access article distributed under the Creative Commons Attribution License, which permits unrestricted use, distribution, and reproduction in any medium, provided the original work is properly cited.

Abstract. With deteriorating infrastructure in many countries on the African continent and declining funding for infrastructure development, diseases such as typhoid fever are a problem. In many of these countries, the disease occurs periodically. This disease, which is caused by *Salmonella Typhi* bacteria, is associated with poor hygiene, poor waste disposal systems and seasonal rains. Recently in Zimbabwe, the infection has been found to exist due to dilapidated infrastructure. The existence of the infection remains a huge public health problem. In this paper, we study the typhoid fever transmission dynamics with fear in periodic environments. We formulate a non-linear system of differential equations in which the infection rate is time dependent. The model's steady states are determined and the stability analysis carried out. Numerical simulations are carried out to determine the impact of the vital parameters on the course of the disease. Sensitivity analysis is also done to determine parameters that influence disease progression the most. The role of fear and seasonality are discussed and the public health implications of the results are articulated.

Keywords: typhoid; fear; seasonality; stability analysis; basic reproduction number.

2010 AMS Subject Classification: 34D20, 34D23, 92B05, 97M10.

*Corresponding author

E-mail address: fnyabadza@uj.ac.za

Received February 22, 2021

1. INTRODUCTION

Typhoid Fever is a life-threatening bacterial infection caused by *Salmonella Typhi* [37]. The transmission mode of typhoid is identical to that of cholera—that is, direct transmission (human-human) and indirect transmission (environment-human). This disease adversely affects the Reticuloendothelial system, the gall bladder and the intestinal lymphoid [23]. Known estimates of the incubation period for the typhoid fever disease range from ten to fourteen days [23]. The case fatality rate of typhoid fever was 10 – 20% before the advent of treatment, whilst, with prompt treatment, the case fatality rate was reduced to less than 1% [13]. It was observed that the number of deaths caused by typhoid fever in the year 1990 was 181 000 [1]; in the year 2000, it was 217 000 [8]; and in the year 2013, it was 161 000 [1]. In the Democratic Republic of Congo, more than 42 000 people contracted the typhoid fever disease during the years 2004 and 2005 [43].

For a number of incurable communicable diseases, modellers typically make the assumption of homogeneous mixing of susceptible and infected individuals in a given population [11]. This assumption is reasonable for most non-lethal infections, such as influenza and chickenpox. However, for lethal infections such as COVID-19, typhoid, cholera and HIV/AIDS this assumption is debatable. In the case of HIV/AIDS, examples of partner preferences can be seen when individuals reduce the number of sexual partners they have, and through stigmatization of those who are already infected [33, 39]. During a cholera, typhoid or COVID-19 outbreak, fear drives individuals to self-isolate and improve personal hygiene in order to reduce the contact rate of these diseases [12, 31, 41]. Indeed, a reduced contact rate, due to fear, has a huge bearing on the dynamics of a lethal infection. The role of fear has been considered in mathematical models with interacting species, see [9, 11, 42]. Recently, the role of fear has been modelled for Ebola virus disease [17]. Very few mathematical models have considered fear as an essential component in human response to infection.

Mathematical models with seasonality have been considered by a number of authors. In [7], a malaria model with seasonality is considered in which a system of differential equations is analysed. A model for malaria was also considered in [38] in with climatic factors where considered

to influence the biting rate. Other infections in which seasonality was considered include brucellosis [26], clostridium difficile [20], schistosomiasis [19], respiratory syncytial virus [21], buruli ulcer [3] and cholera [28]. In these models, seasonality is modelled by incorporating a trigonometric function in the force of infection. It is also common to come across mathematical models for diarrhoeal diseases such as cholera, typhoid and many others that assume a constant rate of infection. The primary reason of making such an assumption is that it makes for relatively easy analysis, in that, it produces models that contain systems of autonomous ordinary differential equations [30]. To this end, there are numerous tools for analysing systems of autonomous ordinary differential equations in the literature [15, 36]. The major drawback of assuming a constant infection rate for a seasonal disease is that the accuracy of the model might be compromised, thus compromising model predictions. Empirically, it has been shown that typhoid fever is highly seasonal and it peaks during the rainy seasons [32], hence a seasonal mathematical model is befitting to study such a disease.

To the best of our knowledge, the dynamics of typhoid fever's seasonality coupled with a behavioural change in the population due to the fear of infection has not been investigated. A comparison of a seasonal mathematical model of typhoid fever and one where the assumption of seasonality is relaxed is carried out. We seek to understand the effects of seasonality on the basic reproduction number, the number of steady states, the stability of these steady states and to carry out the stability analysis of the steady states.

The paper is arranged as follows; in Section 2, we formulate and establish the basic properties of the model. The model is analysed for stability in Section 3. In Section 4, we carry out some numerical simulations. Parameter estimation and numerical results are also presented in this section. The paper is concluded in Section 5.

2. METHODOLOGY

2.1. Model Formulation. The typhoid infection model classifies the total human population at time t , denoted by $N(t)$, into susceptible individuals $S(t)$, typhoid infected individuals $I(t)$, individuals who recovered from typhoid $R(t)$. Thus, $N(t) = S(t) + I(t) + R(t)$. The model has an additional compartment $B(t)$ which represents the *Salmonella Typhi* concentration in the environment. The dynamics of the model developed in this paper follows from the model developed

by Mushanyu *et al.* [22].

We assume that susceptible individuals acquire typhoid fever either through person-to-person transmission or by ingesting *Salmonella Typhi* from contaminated aquatic reservoirs at the rates

$$\lambda_1 = \frac{\beta_{t_1} I}{1 + kI}, \quad \lambda_2 = \frac{\beta_{t_2} B}{\kappa_t + B} \left(1 + \theta \sin \left(\frac{2\pi t}{365} \right) \right),$$

respectively. The parameter β_{t_1} denotes the person-to-person typhoid transmission rate of susceptibles and is defined as the product of the probability of typhoid transmission per contact and the effective contact rate for typhoid transmission to occur. The parameter β_{t_2} denotes the environment-to-humans per capita contact rate for susceptibles and the *Salmonella Typhi* in the contaminated environment and κ_t denotes the half saturation constant relative to the *Salmonella Typhi*. Here, we assume that individuals under treatment are infectious but cannot infect susceptible individuals since they will be confined to a certain place and separated from the general population where they will be released upon successful treatment or due to mortality (natural or disease related).

Infected individuals in class I experience disease related death at a rate given by δ . Individuals in the infectious state I excrete *Salmonella Typhi* bacteria into the environment at rate α . Individuals in the recovered class R are temporarily immune to typhoid infection, and immunity wanes at a rate given by ρ , leading to the individuals being susceptible again.

The *Salmonella Typhi* bacteria population is generated at a rate $g_b B$ and its growth is enhanced by individuals in the infectious state I . We assume that the *Salmonella Typhi* bacteria in the environment becomes non-infectious at a rate μ_b . The constant recruitment into the susceptible population is represented by Λ , while the natural death rate for the general population is represented by μ_h . We assume that individuals in each compartment are indistinguishable and there is homogeneous mixing.

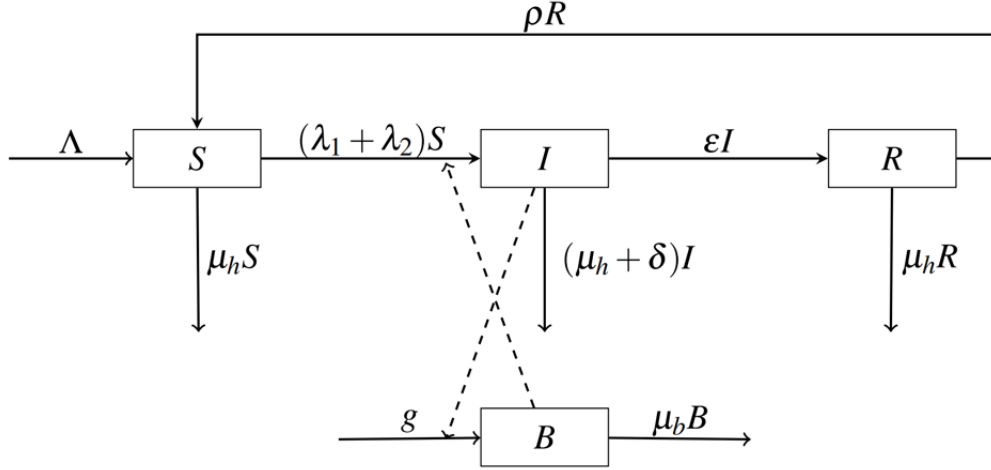


Figure 1. The typhoid compartmental model, where $g = g_b B \left(1 - \frac{B}{k_t}\right) \left(1 + \xi \sin\left(\frac{2\pi t}{365}\right)\right) + \alpha I$.

The schematic diagram for the model to be analysed in this work is given below.

Given the schematic diagram in Fig 1 and the given model assumptions, we formulate the typhoid fever model as follows

$$\begin{aligned}
 \frac{dS}{dt} &= \Lambda - (\lambda_1 + \lambda_2)S - \mu_h S + \rho R, \\
 \frac{dI}{dt} &= (\lambda_1 + \lambda_2)S - qI, \\
 \frac{dR}{dt} &= \epsilon I - (\mu_h + \rho)R, \\
 \frac{dB}{dt} &= g_b B \left(1 - \frac{B}{k_t}\right) \left(1 + \xi \sin\left(\frac{2\pi t}{365}\right)\right) + \alpha I - \mu_b B,
 \end{aligned}
 \tag{1}$$

where $q = \mu_h + \delta + \epsilon$, with initial conditions

$$S(0) = S_0 > 0, \quad B(0) = B_0 \geq 0, \quad I(0) = I_0 \geq 0, \quad R(0) = R_0 \geq 0.$$

2.2. Non-seasonal Typhoid Model. Applying the time-average function, $[f(t)] = \frac{1}{\omega} \int_0^\omega f(t) dt$, to each component of the typhoid model (1) gives the following auxiliary system

$$\begin{aligned}
(2) \quad \frac{dS}{dt} &= \Lambda - (\lambda_1 + [\lambda_2])S - \mu_h S + \rho R, \\
\frac{dI}{dt} &= (\lambda_1 + [\lambda_2])S - qI, \\
\frac{dR}{dt} &= \varepsilon I - (\mu_h + \rho)R, \\
\frac{dB}{dt} &= g_b B \left(1 - \frac{B}{k_t}\right) + \alpha I - \mu_b B,
\end{aligned}$$

with initial conditions

$$S(0) = S_0 > 0, \quad B(0) = B_0 \geq 0, \quad I(0) = I_0 \geq 0, \quad R(0) = R_0 \geq 0.$$

Here $[\lambda_2] = \frac{\beta_{t_2} B}{\kappa_t + B}$.

2.2.1. Non-negative Trajectories and Boundedness. We show that all the trajectories of the dynamical system are non-negative. The approach outlined in Yang *et al.* [44] to show that all the solutions are bounded below by zeros is used in this case.

It is clear that

$$\left. \frac{dS}{dt} \right|_{S=0} = \Lambda + \rho R > 0, \quad \left. \frac{dI}{dt} \right|_{I=0} = [\lambda_2]S \geq 0, \quad \left. \frac{dR}{dt} \right|_{R=0} = \varepsilon I \geq 0, \quad \left. \frac{dB}{dt} \right|_{B=0} = \alpha I \geq 0.$$

Using Lemma 2 of Yang *et al.* [44], it follows that the trajectories of model (2) are all non-negative. The time derivative of the human population is given by

$$\frac{dN}{dt} = \Lambda - \mu_h N - \delta I \leq \Lambda - \mu_h N,$$

This separable differential inequality can be integrated to get the following upper bound for $N(t)$

$$N \leq \frac{\Lambda - M \exp(-\mu_h t)}{\mu_h} \leq \frac{\Lambda}{\mu_h}.$$

This implies that each class containing humans is also bounded above by Λ/μ_h . Since $I \leq N \leq \Lambda/\mu_h$, the bacterial class produces the following differential inequality

$$(3) \quad \frac{dB}{dt} = g_b B \left(1 - \frac{B}{k_t}\right) + \alpha I - \mu_b B \leq g_b B \left(1 - \frac{B}{k_t}\right) + \alpha \frac{\Lambda}{\mu_h} - \mu_b B.$$

From inequality (3), if

$$(4) \quad B \geq \alpha \frac{\Lambda}{\mu_h},$$

then

$$(5) \quad \frac{dB}{dt} \leq (g_b - \mu_b)B - \frac{g_b}{k_t}B^2 + B = (g_b - \mu_b + 1)B \left(1 - \frac{g_b B}{k_t(g_b - \mu_b + 1)} \right).$$

Note that the differential inequality (5) is a derivative of the logistic growth model with carrying capacity

$$(6) \quad \frac{k_t(g_b - \mu_b + 1)}{g_b}.$$

On the other hand, if condition (4) is false, then B is bounded above by the constant $\alpha\Lambda/\mu_h$ for some $t \geq 0$. For the rest of the time points in the domain of B , condition (4) is true, and hence the upper bound for B is (6). Thus, in both cases,

$$B \leq \max \left\{ \frac{k_t(g_b - \mu_b + 1)}{g_b}, \alpha \frac{\Lambda}{\mu_h} \right\}.$$

The results on positivity and boundedness of the solutions to the typhoid model (2) can be summarized within the feasible region $\Omega \subseteq \Omega_c$, where

$$\Omega_c = \left\{ (S, I, R, B) \in \mathbb{R}^4 \mid 0 \leq S, I, R \leq \frac{\Lambda}{\mu_h}, 0 \leq B \leq \max \left\{ \frac{k_t(g_b - \mu_b + 1)}{g_b}, \alpha \frac{\Lambda}{\mu_h} \right\} \right\}.$$

Theorem 1. *All solutions of the typhoid model (2) are positively invariant and bounded within Ω .*

2.2.2. Disease Free Equilibrium and Time Average Reproduction Number, ($[\mathcal{R}]_0$). The disease free equilibrium for system (2) is

$$(7) \quad \mathbf{x}_0 = (S, I, R, B) = \left(\frac{\Lambda}{\mu_h}, 0, 0, 0 \right).$$

The basic reproduction number, $[\mathcal{R}_0]$, is defined as the spectral radius of the next generation matrix [10] or given a completely susceptible population, an alternative definition of the basic reproduction number is the average number of secondary infections that arise out of an average primary case [18].

The new infections vector $[\mathcal{F}]$, transmission vector $[\mathcal{V}]$, and their respective Jacobians $[F]$ and $[V]$ are

$$[\mathcal{F}] = \begin{pmatrix} (\lambda_1 + \lambda_2)S \\ 0 \end{pmatrix}, [\mathcal{V}] = \begin{pmatrix} qI \\ \mu_b B - g_b B \left(1 - \frac{B}{k_r}\right) - \alpha I \end{pmatrix}, [F] = \begin{pmatrix} \frac{\Lambda\beta_{t_1}}{\mu_h} & \frac{\Lambda\beta_{t_2}}{\mu_h \kappa_r} \\ 0 & 0 \end{pmatrix}, [V] = \begin{pmatrix} q & 0 \\ -\alpha & \mu_b - g_b \end{pmatrix},$$

since the time average of $\left(1 + \theta \sin\left(\frac{2\pi t}{365}\right)\right)$ is one. Thus the spectral radius of the matrix

$$[F][V]^{-1} = \begin{pmatrix} \frac{\Lambda\beta_{t_1}}{q\mu_h} + \frac{\beta_{t_2}\alpha\Lambda}{q\kappa_r\mu_h(\mu_b - g_b)} & \frac{\beta_{t_2}\Lambda}{\kappa_r\mu_h(\mu_b - g_b)} \\ 0 & 0 \end{pmatrix}$$

is

$$[\mathcal{R}_0] = \frac{\Lambda\beta_{t_1}}{q\mu_h} + \frac{\beta_{t_2}\alpha\Lambda}{q\kappa_r\mu_h(\mu_b - g_b)},$$

where $[\mathcal{R}_0]$ is the so-called *time-averaged basic reproduction number* for the typhoid model (2). It follows that $\mu_b > g_b$ implies $[\mathcal{R}_0] > 0$.

2.2.3. Local Stability Analysis of the Disease Free Equilibrium. We begin by analysing the stability of the solutions of model (2) at the disease free equilibrium \mathbf{x}_0 . We apply the Routh-Hurwitz criterion [14] in order to find the nature of the eigenvalues.

Theorem 2. *The disease free equilibrium, \mathbf{x}_0 , for system (2) is locally asymptotically stable whenever $\mu_b > g_b$ and $[\mathcal{R}_0] < 1$. It is unstable otherwise.*

Proof. The Jacobian of system (2) at the disease free equilibrium is

$$J(\mathbf{x}_0) = \begin{pmatrix} -\mu_h & -\frac{\Lambda\beta_{t_1}}{\mu_h} & \rho & -\frac{\Lambda\beta_{t_2}}{\mu_h \kappa_r} \\ 0 & \frac{\Lambda\beta_{t_1}}{\mu_h} - q & 0 & \frac{\Lambda\beta_{t_2}}{\mu_h \kappa_r} \\ 0 & \varepsilon & -(\mu_h + \rho) & 0 \\ 0 & \alpha & 0 & g_b - \mu_b \end{pmatrix}.$$

By inspection, it is clear that the two eigenvalues, $-\mu_h$ and $-(\mu_h + \rho)$, of $J(\mathbf{x}_0)$ lie in the left open half plane. The properties of the remaining two eigenvalues will be obtained from the

following sub-matrix

$$\bar{J}(\mathbf{x}_0) = \begin{pmatrix} \frac{\Lambda\beta_{t_1}}{\mu_h} - q & \frac{\Lambda\beta_{t_2}}{\mu_h\kappa_t} \\ \alpha & g_b - \mu_b \end{pmatrix}.$$

The characteristic polynomial associated with matrix $\bar{J}(\mathbf{x}_0)$ is $\lambda^2 - tr(\bar{J}(\mathbf{x}_0))\lambda + det(\bar{J}(\mathbf{x}_0))$.

The Routh-Hurwitz criterion states that the roots of $\bar{J}(\mathbf{x}_0)$ lie in the left open half plane if and only if $tr(\bar{J}(\mathbf{x}_0)) < 0$ and $det(\bar{J}(\mathbf{x}_0)) > 0$. Indeed,

$$tr(\bar{J}(\mathbf{x}_0)) = \frac{\Lambda\beta_{t_1}}{\mu_h} - q + g_b - \mu_b = q \left(\frac{\Lambda\beta_{t_1}}{\mu_h q} - 1 + \frac{g_b - \mu_b}{q} \right),$$

$$det(\bar{J}(\mathbf{x}_0)) = q(g_b - \mu_b) \left(\frac{\Lambda\beta_{t_1}}{\mu_h q} - 1 + \frac{\alpha\Lambda\beta_{t_2}}{\mu_h\kappa_t q(\mu_b - g_b)} \right) = q(\mu_b - g_b)(1 - [\mathcal{R}_0]).$$

We observe that $tr(\bar{J}(\mathbf{x}_0)) < 0$ if $\mu_b > g_b$ and $\frac{\Lambda\beta_{t_1}}{\mu_h q} < 1$, whilst $det(\bar{J}(\mathbf{x}_0)) > 0$ if $\mu_b > g_b$ and $[\mathcal{R}_0] < 1$. It is also worth noting that $[\mathcal{R}_0] < 1$ implies $\frac{\Lambda\beta_{t_1}}{\mu_h q} < 1$. Thus $tr(\bar{J}(\mathbf{x}_0)) < 0$ and $det(\bar{J}(\mathbf{x}_0)) > 0$ whenever $\mu_b > g_b$ and $[\mathcal{R}_0] < 1$. Therefore, it follows from the Routh-Hurwitz criterion that $\mu_b > g_b$ and $[\mathcal{R}_0] < 1$ implies that all four eigenvalues of $J(\mathbf{x}_0)$ lie in the left open half plane. \square

2.2.4. Global Stability Analysis of the Disease Free Equilibrium. Following Bhunu *et al.* [4], we study the global stability of the system by casting the system into the following form

$$\frac{d\mathbf{X}}{dt} = \mathbf{F}(\mathbf{X}, \mathbf{Y}), \quad \frac{d\mathbf{Y}}{dt} = \mathbf{G}(\mathbf{X}, \mathbf{Y}), \quad \mathbf{G}(\mathbf{X}^*, \mathbf{0}) = \mathbf{0},$$

where $\mathbf{X} = (S, R)$ and $\mathbf{Y} = (I, B)$. The disease free equilibrium is then written in the form

$$\mathbf{U}_0 = (\mathbf{X}^*, \mathbf{0}), \quad \mathbf{X}^* = \left(\frac{\Lambda}{\mu_h}, \mathbf{0} \right).$$

The conditions that must be met in order for the system to be globally asymptotically stable are:

$$(H1) \quad \frac{d\mathbf{X}}{dt} = \mathbf{F}(\mathbf{X}^*, \mathbf{0}), \quad \mathbf{X}^* \text{ is globally asymptotically stable,}$$

$$(H2) \quad \mathbf{G}(\mathbf{X}, \mathbf{Y}) = \mathbf{A}\mathbf{Y} - \hat{\mathbf{G}}(\mathbf{X}, \mathbf{Y}), \quad \hat{\mathbf{G}}(\mathbf{X}, \mathbf{Y}) \geq \mathbf{0} \quad \text{for } (\mathbf{X}, \mathbf{Y}) \in \Omega,$$

where $\mathbf{A} = D_{\mathbf{Y}} \mathbf{G}(\mathbf{X}^*, \mathbf{0})$ is a Metzler matrix, and Ω is the region of biological significance.

Theorem 3. ([6], p. 19) *The fixed point $\mathbf{U}_0 = (\mathbf{X}^*, \mathbf{0})$ is a globally asymptotically stable equilibrium of a system provided that $[\mathcal{R}_0] < 1$, and conditions (H1) and (H2) are satisfied.*

We establish the global stability of system (2) following Theorem (3).

Theorem 4. *The disease free equilibrium of the typhoid model (2) is globally asymptotically stable if $[\mathcal{R}_0] < 1$.*

Proof. Applying condition (H1) to the system gives

$$(8) \quad \frac{d\mathbf{X}}{dt} = \mathbf{F}(\mathbf{X}^*, \mathbf{0}) = \begin{pmatrix} \Lambda - \mu_h S + \rho R \\ -(\mu_h + \rho)R \end{pmatrix}.$$

The Jacobian of equation (8) is

$$D_{\mathbf{X}} \mathbf{F}(\mathbf{X}^*, \mathbf{0}) = \begin{pmatrix} -\mu_h & \rho \\ 0 & -(\mu_h + \rho) \end{pmatrix}.$$

We conclude that the fixed point \mathbf{X}^* is a globally asymptotically stable equilibrium point of system (8) since the system is linear, and all the eigenvalues of the Jacobian are negative and real. Alternatively, the solution for system (8) is

$$\mathbf{X} = c_1 \exp(-ut) \mathbf{e}_1 + c_2 \exp(-(u + \rho)t) (\mathbf{e}_1 - \mathbf{e}_2) + \frac{\Lambda}{\mu_h} \mathbf{e}_1,$$

where $\{\mathbf{e}_1, \mathbf{e}_2\}$ is the standard basis in \mathbb{E}^2 . Thus, $\lim_{t \rightarrow \infty} \mathbf{X} = \mathbf{X}^*$.

Applying condition (H2) to the system yields

$$[A] = \begin{pmatrix} \frac{\Lambda}{\mu_h} \beta_{t_1} - q & \frac{\beta_{t_2} \Lambda}{\kappa_t \mu_h} \\ \alpha & g_b - \mu_b \end{pmatrix}, \quad [\hat{\mathbf{G}}] = \begin{pmatrix} \beta_{t_1} I \left(\frac{\Lambda}{\mu_h} - \frac{S}{1+kI} \right) + \beta_{t_2} B \left(\frac{\Lambda}{\kappa_t \mu_h} - \frac{S}{B + \kappa_t} \right) \\ \frac{g_b}{\kappa_t} B^2 \end{pmatrix}.$$

Since $1/(1+kI) \leq 1$ and $S \leq \Lambda/\mu_h$, it follows that $S/(1+kI) \leq \Lambda/\mu_h$ or $\Lambda/\mu_h - S/(1+kI) \geq 0$. Also, since $B/(B + \kappa_t) \leq 1/\kappa_t$, because $B > 0$, and $S \leq \Lambda/\mu_h$, it follows that $S/(B + \kappa_t) \leq \Lambda/\mu_h \kappa_t$ or $\Lambda/\mu_h \kappa_t - S/(B + \kappa_t) \geq 0$. We conclude that $\hat{\mathbf{G}}(\mathbf{X}, \mathbf{Y}) \geq \mathbf{0}$ in the biologically feasible region Ω . Since system (2) satisfies conditions (H1) and (H2), it follows from Theorem (3) that $[\mathcal{R}_0] < 1$ implies that the disease free equilibrium for system (2) is globally asymptotically stable. \square

2.2.5. Endemic Equilibrium. The endemic equilibrium for the typhoid model (2) is given by setting the time derivative for each class to zero.

$$\begin{aligned}\Lambda - (\lambda_1^* + \lambda_2^*)S^* - \mu_h S^* + \rho R^* &= 0, & (\lambda_1^* + \lambda_2^*)S^* - qI^* &= 0, \\ \varepsilon I^* - (\mu_h + \rho)R^* &= 0, & g_b B^* \left(1 - \frac{B^*}{k_t}\right) + \alpha I^* - \mu_b B^* &= 0.\end{aligned}$$

We isolate R^* and S^* from $\varepsilon I^* - (\mu_h + \rho)R^* = 0$ and $(\lambda_1^* + \lambda_2^*)S^* - qI^* = 0$, respectively. We then substitute those expressions for $R^* = \varepsilon I^*/(\mu_h + \rho)$ and $S^* = qI^*/(\lambda_1^* + \lambda_2^*)$ into $\Lambda - (\lambda_1^* + \lambda_2^*)S^* - \mu_h S^* + \rho R^* = 0$ to produce

$$\Lambda - qI^* - \frac{\mu_h q I^*}{\lambda_1^* + \lambda_2^*} + \frac{\rho \varepsilon I^*}{\mu_h + \rho} = \Lambda + \left(\frac{(\lambda_1^* + \lambda_2^*)\rho \varepsilon - q(\mu_h + \rho)(\lambda_1^* + \lambda_2^* + \mu_h)}{(\mu_h + \rho)(\lambda_1^* + \lambda_2^*)} \right) I^* = 0.$$

Isolation of I^* gives

$$(9) \quad I^* = \frac{\Lambda(\mu_h + \rho)(\lambda_1^* + \lambda_2^*)}{(\lambda_1^* + \lambda_2^*)(\rho(\mu_h + \delta) + \mu_h q) + \mu_h q(\mu_h + \rho)}.$$

Back substituting equation (9) into $R^* = \varepsilon I^*/(\mu_h + \rho)$ and $S^* = qI^*/(\lambda_1^* + \lambda_2^*)$, respectively, gives

$$R^* = \frac{\varepsilon \Lambda (\lambda_1^* + \lambda_2^*)}{(\lambda_1^* + \lambda_2^*)(\rho(\mu_h + \delta) + \mu_h q) + \mu_h q(\mu_h + \rho)}, \quad S^* = \frac{q \Lambda (\mu_h + \rho)}{(\lambda_1^* + \lambda_2^*)(\rho(\mu_h + \delta) + \mu_h q) + \mu_h q(\mu_h + \rho)}.$$

In order to show the existence of the endemic equilibrium for the typhoid model (2), we complete the square on the equation: $g_b B^* \left(1 - \frac{B^*}{k_t}\right) + \alpha I^* - \mu_b B^* = 0$, to obtain

$$(10) \quad \left(B^* + \frac{k_t(\mu_b - g_b)}{2g_b} \right)^2 = \frac{k_t^2(\mu_b - g_b)^2 + 4g_b k_t \alpha I^*}{4g_b^2}.$$

The two roots for the equation (10) are

$$B^{(1)} = \frac{-k_t(\mu_b - g_b) + \sqrt{k_t^2(\mu_b - g_b)^2 + 4g_b k_t \alpha I^*}}{2g_b}, \quad B^{(2)} = \frac{-k_t(\mu_b - g_b) - \sqrt{k_t^2(\mu_b - g_b)^2 + 4g_b k_t \alpha I^*}}{2g_b}.$$

Since $k_t^2(\mu_b - g_b)^2 \leq k_t^2(\mu_b - g_b)^2 + 4g_b k_t \alpha I^*$, it follows from taking the square root function on both sides of the inequality that $k_t|\mu_b - g_b| \leq \sqrt{k_t^2(\mu_b - g_b)^2 + 4g_b k_t \alpha I^*}$, therefore $-\sqrt{k_t^2(\mu_b - g_b)^2 + 4g_b k_t \alpha I^*} \leq k_t(\mu_b - g_b) \leq \sqrt{k_t^2(\mu_b - g_b)^2 + 4g_b k_t \alpha I^*}$. Hence subtracting $k_t(\mu_b - g_b)$ from the inequalities and then dividing by $2g_b$ yields $B^{(2)} \leq 0 \leq B^{(1)}$. Clearly, $B^{(2)}$ must be discarded since it is negative, thus $B^* = B^{(1)}$.

2.3. The Seasonal Typhoid Model. We study the full effects of seasonality on the typhoid model by removing the time-average function, $[f(t)] = \frac{1}{\omega} \int^{\omega} f(t) dt$, from our analysis. We apply our analysis on model (1) for the rest of this section. The model with seasonality thus becomes non-autonomous.

2.3.1. Properties of the non-autonomous model. We show that model (1) is well posed, it has non-negative trajectories, a unique disease free equilibrium, among others. Setting all the derivatives of dynamical system (1) to zeros, and setting $(I, B) = (0, 0)$, gives a unique disease free equilibrium $(S^*, I^*, R^*, B^*) = (\Lambda/\mu_h, 0, 0, 0)$.

Since $\lambda_1, \lambda_2 \geq 0$, it follows that $\lambda_1 + \lambda_2 \geq 0$. We conclude that the force of infection for model (1) is non-negative.

The partial derivatives of the force of infection are

$$\frac{\partial}{\partial I} (\lambda_1 + \lambda_2) = \frac{\beta_{t_1}}{(1+kI)^2} \geq 0, \quad \frac{\partial}{\partial B} (\lambda_1 + \lambda_2) = \frac{\beta_{t_2} \kappa_t}{(B + \kappa_t)^2} \left(1 + \theta \sin \left(\frac{2\pi t}{365} \right) \right) \geq 0.$$

It is clear that the force of infection increases with the number of infected people and the concentration of bacteria. The bacterial growth rates are bounded as follows:

$$\frac{\partial}{\partial B} \left(\frac{dB}{dt} \right) = g_b \left(1 - 2 \frac{B}{k_t} \right) \left(1 + \xi \sin \left(\frac{2\pi t}{365} \right) \right) - \mu_b \leq 0, \quad \frac{\partial}{\partial I} \left(\frac{dB}{dt} \right) = \alpha \geq 0,$$

whenever $B \geq k_t/2$. The first inequality shows that the bacterial growth rate increases with the number of infected individuals; the second inequality shows that in the absence of infected people, there exists a threshold, $k_t/2$, such that if the bacteria exceeds this threshold, then the bacterial growth rate decreases with the concentration of the bacteria.

We show, geometrically, that the surface that represents the force of infection, $\lambda_1 + \lambda_2$, lies below its associated tangent plane at the origin. This means that the remainder term, R_1 , from the truncated Taylor expansion of $\lambda_1 + \lambda_2$ when the degree equals one is non-positive. The second partial derivatives of the force of infection are

$$\frac{\partial^2}{\partial I^2} (\lambda_1 + \lambda_2) = \frac{-2\beta_{t_1} k}{(1+kI)^3} \leq 0, \quad \frac{\partial^2}{\partial B \partial I} (\lambda_1 + \lambda_2) = 0, \quad \frac{\partial^2}{\partial B^2} (\lambda_1 + \lambda_2) = \frac{-2\beta_{t_2} \kappa_t}{(B + \kappa_t)^3} \left(1 + \theta \sin \left(\frac{2\pi t}{365} \right) \right) \leq 0.$$

Consider the matrix

$$A = \begin{bmatrix} \frac{\partial^2}{\partial I^2} (\lambda_1 + \lambda_2) & \frac{\partial^2}{\partial B \partial I} (\lambda_1 + \lambda_2) \\ \frac{\partial^2}{\partial B \partial I} (\lambda_1 + \lambda_2) & \frac{\partial^2}{\partial B^2} (\lambda_1 + \lambda_2) \end{bmatrix} = \begin{bmatrix} \frac{-2\beta_{t_1} k}{(1+kI)^3} & 0 \\ 0 & \frac{-2\beta_{t_2} \kappa_t}{(B + \kappa_t)^3} \left(1 + \theta \sin \left(\frac{2\pi t}{365} \right) \right) \end{bmatrix}.$$

Since

$$\begin{bmatrix} I \\ B \end{bmatrix}^T \begin{bmatrix} \frac{-2\beta_1 k}{(1+kI)^3} & 0 \\ 0 & \frac{-2\beta_2 \kappa_t}{(B+\kappa_t)^3} \left(1 + \theta \sin\left(\frac{2\pi t}{365}\right)\right) \end{bmatrix} \begin{bmatrix} I \\ B \end{bmatrix} = -2 \left(\frac{\beta_1 k I^2}{(1+kI)^3} + \frac{\beta_2 \kappa_t B^2}{(B+\kappa_t)^3} \left(1 + \theta \sin\left(\frac{2\pi t}{365}\right)\right) \right) \leq 0,$$

$$R_1 = - \left(\frac{\beta_1 k \zeta^2}{(1+k\zeta)^3} + \frac{\beta_2 \kappa_t \eta^2}{(\eta + \kappa_t)^3} \left(1 + \theta \sin\left(\frac{2\pi t}{365}\right)\right) \right),$$

where $\zeta \in (0, I)$ and $\eta \in (0, B)$, it follows that $R_1 \leq - \left(\frac{\beta_1 k I^2}{(1+kI)^3} + \frac{\beta_2 \kappa_t B^2}{(B+\kappa_t)^3} \left(1 + \theta \sin\left(\frac{2\pi t}{365}\right)\right) \right) \leq 0$, and that matrix A is negative semi-definite.

It is clear to see that $I > 0$ implies $\lambda_1 + \lambda_2 > 0$ and $B > 0$ implies $\lambda_1 + \lambda_2 > 0$. The model shows that in the absence of bacteria, a single infected individual is sufficient for a positive infection rate; and in the absence of infected individuals, the presence of bacteria is sufficient for a positive infection rate.

2.3.2. Basic Reproduction Number. We apply the methods outlined in [35, 40] to determine basic reproduction number.

We show that the system (1) meets the seven assumptions in the article by Wang and Zhao [40]. Let $\mathbf{x} = (S, I, R, B)^T$. The disease free equilibrium is $\mathbf{x}_0 = (\Lambda/\mu_h, 0, 0, 0)^T$ and the new infections vector and transfer vectors are as follows

$$\mathcal{F} = \begin{pmatrix} (\lambda_1 + \lambda_2)S \\ 0 \\ 0 \\ 0 \end{pmatrix}, \quad \mathcal{V}^- = \begin{pmatrix} qI \\ \mu_b B \\ (\lambda_1 + \lambda_2)S + \mu_h S \\ (\mu_h + \rho)R \end{pmatrix}, \quad \mathcal{V}^+ = \begin{pmatrix} 0 \\ g_b B \left(1 - \frac{B}{\kappa_t}\right) \left(1 + \xi \sin\left(\frac{2\pi t}{365}\right)\right) + \alpha I \\ \Lambda + \rho R \\ \epsilon I \end{pmatrix}.$$

The Jacobians of the input rate of new infections and the transfer rate of infections are

$$F(t) = \begin{pmatrix} \frac{\Lambda}{\mu_h} \beta_{t_1} & \frac{\Lambda \beta_{t_2}}{\mu_h \kappa_t} \left(1 + \theta \sin\left(\frac{2\pi t}{365}\right)\right) \\ 0 & 0 \end{pmatrix}, \quad V(t) = \begin{pmatrix} q & 0 \\ -\alpha & \mu_b - g_b \left(1 + \xi \sin\left(\frac{2\pi t}{365}\right)\right) \end{pmatrix}.$$

Define $f = \mathcal{F} - \mathcal{V}$, $\mathcal{V} = \mathcal{V}^- - \mathcal{V}^+$, and $\rho(J)$ as the spectral radius of matrix J .

Lemma 1. ([45], Lemma 2.1.) *Let $A(t)$ be a continuous, cooperative, irreducible, and ω -periodic $k \times k$ matrix function and let $p = \frac{1}{\omega} \ln(\rho(\Phi_A(\omega)))$. Then*

$$(11) \quad \frac{d\mathbf{x}(t)}{dt} = A(t)\mathbf{x}(t),$$

gives a solution $\mathbf{x}(t) = e^{Pt} \mathbf{v}(t)$ for some ω -periodic function $\mathbf{v}(t)$. $\Phi_A(\omega)$ denotes the monodromy matrix of system (11).

The next infection operator is defined by [40] as follows

$$(12) \quad (L\phi) = \int_0^\infty Y(t, t-s)F(t-s)\phi(t-s)ds,$$

where $Y(t, s)$ is the evolution operator for the system $dy/dt = -V(t)y$ and $\phi(t)$ is the initial distribution function of the infected. The spectral radius of L gives the basic reproduction number

$$\mathcal{R}_0 = \rho(L).$$

In most nonlinear systems, the integral in equation (12) is intractable, thus numerical methods are used to compute \mathcal{R}_0 . Since the basic reproduction number is the maximum eigenvalue of the operator eigenvalue problem $(L\phi)t = \lambda\phi(t)$, the authors of [29] constructed an eigenvalue-preserving transformation of the above operator eigenvalue problem into a matrix eigenvalue problem. The spectral radius of the eigenvalue problem is an accurate estimator for the true basic reproduction number.

Theorem 5. ([40], Theorem 2.2) *The following statements are valid for model (1):*

1. $\mathcal{R}_0 = 1 \iff \rho(\Phi_f(365)) = 1,$
2. $\mathcal{R}_0 < 1 \iff \rho(\Phi_f(365)) < 1,$
3. $\mathcal{R}_0 > 1 \iff \rho(\Phi_f(365)) > 1,$
4. $\mathcal{R}_0 < 1$ ($\mathcal{R}_0 > 1$) $\implies \mathbf{x}_0$ is locally asymptotically stable (unstable),

whenever,

(B1) *The functions $\mathcal{F}(t, \mathbf{x}) \geq 0$, $\mathcal{V}^+(t, \mathbf{x}) \geq 0$, and $\mathcal{V}^-(t, \mathbf{x}) \geq 0$ are continuous, continuously differentiable with respect to x on $\mathbb{R} \times \mathbb{R}_+^4$, and each have a period of 365 with respect to t .*

(B2) $\mathbf{x}_i = 0 \implies \mathcal{V}_i^-$ for $i = 1, 2$.

(B3) $i > 2 \implies \mathcal{F}_i = 0$.

(B4) $\mathcal{F}_i(\mathbf{x}_0) = 0 \wedge \mathcal{V}_i^+(\mathbf{x}_0) = 0$ for $i = 1, 2$.

(B5) $\rho(\Phi_f(365)) < 1$, where $\rho(\Phi_f(365))$ is the spectral radius of $\Phi_f(365)$.

$$(B6) \quad \rho(\Phi_{-V}(365)) < 1$$

We claim that, for model (1), f conditionally satisfies (B1) to (B6). By inspection, we can see that for each $i = 1, \dots, 4$, the functions $\mathcal{F}_i(t, \mathbf{x})$, $\mathcal{V}_i^+(t, \mathbf{x})$, and $\mathcal{V}_i^-(t, \mathbf{x})$ are non-negative, continuous on $\mathbb{R} \times \mathbb{R}_+^4$, continuously differentiable with respect to \mathbf{x} , and 365-periodic in t . If $I = 0$ ($B = 0$), then $\mathcal{V}_1^-(t, \mathbf{x}) = 0$ ($\mathcal{V}_2^-(t, \mathbf{x}) = 0$). $\mathcal{F}_3(t, \mathbf{x}) = \mathcal{F}_4(t, \mathbf{x}) = 0$. At the disease free state, \mathbf{x}_0 , for each $i = 1, 2$, $\mathcal{F}_i(t, \mathbf{x}) = \mathcal{V}_i^+(t, \mathbf{x}) = 0$. We define the matrix

$$M(t) = \left[\frac{\partial}{\partial x_j} \left(f_i(t, \mathbf{x}_0) \right) \right]_{3 \leq i, j \leq 4} = \begin{bmatrix} -\mu_h & \rho \\ 0 & -(\mu_h + \rho) \end{bmatrix},$$

where $f_i(t, \mathbf{x}_0) = \mathcal{F}_i(t, \mathbf{x}) - (\mathcal{V}_i^-(t, \mathbf{x}) - \mathcal{V}_i^+(t, \mathbf{x}))$. The initial value problem, $\mathbf{z}' = M\mathbf{z}$, $\mathbf{z}(s, s) = I_{2 \times 2}$, can be written component wise to produce the system

$$\frac{dz_1}{dt} = -\mu_h z_1 + \rho z_3, \quad \frac{dz_2}{dt} = -\mu_h z_2 + \rho z_4, \quad \frac{dz_3}{dt} = -(\mu_h + \rho) z_3, \quad \frac{dz_4}{dt} = -(\mu_h + \rho) z_4.$$

The solution and the monodromy matrices to the initial value problem above are, respectively,

$$(13) \quad z(t, s) = \begin{bmatrix} \exp(\mu_h(s-t)) & \exp(\mu_h(s-t)) - \exp((\mu_h + \rho)(s-t)) \\ 0 & \exp((\mu_h + \rho)(s-t)) \end{bmatrix},$$

$$z(t, 0) = \Phi_M(t) = \begin{bmatrix} \exp(-\mu_h t) & \exp(-\mu_h t) - \exp(-(\mu_h + \rho)t) \\ 0 & \exp(-(\mu_h + \rho)t) \end{bmatrix}.$$

The spectral radius of the monodromy matrix (13) at $t = 365$ is

$$\rho(\Phi_M(365)) = \max\{\exp(-365\mu_h), \exp(-365(\mu_h + \rho))\} < 1.$$

The initial value problem $\mathbf{Y}' = -V(t)\mathbf{Y}$, $\mathbf{Y}(s, s) = I_{2 \times 2}$, can be written component wise as follows

$$\frac{d}{dt} \left(Y_1(t, s) \right) = -qY_1(t, s), \quad \frac{d}{dt} \left(Y_2(t, s) \right) = -qY_2(t, s),$$

$$\frac{d}{dt} \left(Y_3(t, s) \right) = \alpha Y_1(t, s) + \left(\left(1 + \xi \sin \left(\frac{2\pi t}{365} \right) \right) g_b - \mu_b \right) Y_3(t, s),$$

$$\frac{d}{dt} \left(Y_4(t, s) \right) = \alpha Y_2(t, s) + \left(\left(1 + \xi \sin \left(\frac{2\pi t}{365} \right) \right) g_b - \mu_b \right) Y_4(t, s).$$

Thus a solution to the differential equation

$$(14) \quad \frac{d}{dt} \left(Y(t, s) \right) = -V(t)Y(t, s), \quad \forall t \geq s, \quad Y(s, s) = I_{2 \times 2},$$

is

$$Y(t, s) = \begin{bmatrix} Y_1(t, s) & Y_2(t, s) \\ Y_3(t, s) & Y_4(t, s) \end{bmatrix} = \begin{bmatrix} \exp(q(s-t)) & 0 \\ Y_3(t, s) & \exp \left((g_b - \mu_b)(t-s) + \xi g_b \frac{365}{2\pi} \left(\cos \left(\frac{2\pi s}{365} \right) - \cos \left(\frac{2\pi t}{365} \right) \right) \right) \end{bmatrix},$$

where

$$Y_3(t, s) = \alpha \exp \left(qs + (g_b - \mu_b)t - \frac{365}{2\pi} \xi g_b \cos \left(\frac{2\pi t}{365} \right) \right) \int_s^t \exp \left((\mu_b - g_b - q)\tau + \frac{365}{2\pi} \xi g_b \cos \left(\frac{2\pi \tau}{365} \right) \right) d\tau.$$

The monodromy matrix of differential equation (14) is

$$\Phi_{-V}(t) = Y(t, 0) = \begin{bmatrix} \exp(-qt) & 0 \\ Y_3(t, 0) & \exp \left((g_b - \mu_b)t + \xi g_b \frac{365}{2\pi} \left(1 - \cos \left(\frac{2\pi t}{365} \right) \right) \right) \end{bmatrix}.$$

Thus, the spectral radius is $\rho(\Phi_{-V}(365)) = \max\{\exp(-365q), \exp(365(g_b - \mu_b))\}$. It is clear to see that $\rho(\Phi_{-V}(365)) < 1$ whenever $g_b < \mu_b$. We have proven that assumptions (A1)—(A7) of Wang [40] hold for model (1) if $g_b < \mu_b$.

Corollary 5.1. *The following statements are valid for model (1) if $g_b < \mu_b$:*

- (I) $\mathcal{R}_0 = 1 \iff \rho(\Phi_f(365)) = 1$.
- (II) $\mathcal{R}_0 < 1 \iff \rho(\Phi_f(365)) < 1$.
- (III) $\mathcal{R}_0 > 1 \iff \rho(\Phi_f(365)) > 1$.
- (IV) *The disease free equilibrium, \mathbf{x}_0 , is locally asymptotically stable if $\mathcal{R}_0 < 1$, and unstable if $\mathcal{R}_0 > 1$.*

Proof. Since model (1) satisfies conditions (A1)—(A7) of Wang [40] whenever $g_b < \mu_b$, it follows from Theorem 2.2 of [40] that $g_b < \mu_b$ implies that conditions (I) – (IV) hold. \square

2.3.3. Global Stability of the Disease Free Equilibrium. In this subsection, we prove that the disease free equilibrium of model (1) is globally asymptotically stable. We begin with the following Theorem.

Theorem 6. ([34], *Theorem B.1.*) *Let $D \subseteq \mathbb{R}^n$ be open in \mathbb{R}^n . Let $f : \mathbb{R} \times D \rightarrow \mathbb{R}^n$ be continuous on $\mathbb{R} \times D$ such that. Let $x(t)$ be a solution of (B.1) defined on $[a, b]$. If $z(t)$ is a continuous function on $[a, b]$ satisfying (B.2) on (a, b) with $z(a) \leq x(a)$, then $z(t) \leq x(t)$ for all t in $[a, b]$. If $y(t)$ is continuous on $[a, b]$ satisfying (B.3) on (a, b) with $y(a) \geq x(a)$, then $y(t) \geq x(t)$ for all t in $[a, b]$.*

Limiting our focus to the two infected classes, I and B , the Jacobian of system (1) is

$$[F(t) - V(t)] = \begin{bmatrix} \frac{\Lambda}{\mu_h} \beta_{t_1} - q & \frac{\Lambda \beta_{t_2}}{\mu_h k_t} \left(1 + \theta \sin \left(\frac{2\pi t}{365} \right) \right) \\ \alpha & g_b \left(1 + \xi \sin \left(\frac{2\pi t}{365} \right) \right) - \mu_b \end{bmatrix}.$$

Applying Lemma (1) to $\mathbf{z} = [\tilde{I}_t, \tilde{B}_t]^T$ gives

$$\frac{d}{dt} \begin{bmatrix} \tilde{I}_t \\ \tilde{B}_t \end{bmatrix} = \begin{bmatrix} \frac{\Lambda}{\mu_h} \beta_{t_1} - q & \frac{\Lambda \beta_{t_2}}{\mu_h k_t} \left(1 + \theta \sin \left(\frac{2\pi t}{365} \right) \right) \\ \alpha & g_b \left(1 + \xi \sin \left(\frac{2\pi t}{365} \right) \right) - \mu_b \end{bmatrix} \begin{bmatrix} \tilde{I}_t \\ \tilde{B}_t \end{bmatrix} \implies \begin{bmatrix} \tilde{I}_t \\ \tilde{B}_t \end{bmatrix} = e^{bt} \mathbf{v}(t).$$

Since $\mathcal{R}_0 < 1 \iff \rho(\Phi_f(365)) < 1 \iff b < 0$, it follows that $\mathcal{R}_0 < 1$ implies $\lim_{t \rightarrow \infty} e^{bt} \mathbf{v}(t) = [0, 0]^T$. From applying the Taylor expansion to first order and using the $R_1 \leq 0$, we obtain the following differential inequality

$$\begin{aligned} \frac{d}{dt} \begin{bmatrix} I \\ B \end{bmatrix} &= \begin{bmatrix} (\lambda_1 + \lambda_2)S - qI \\ g_b B \left(1 - \frac{B}{k_t} \right) \left(1 + \xi \sin \left(\frac{2\pi t}{365} \right) \right) + \alpha I - \mu_b B \end{bmatrix}, \\ &= \begin{bmatrix} \frac{\Lambda}{\mu_h} \beta_{t_1} - q & \frac{\Lambda \beta_{t_2}}{\mu_h k_t} \left(1 + \theta \sin \left(\frac{2\pi t}{365} \right) \right) \\ \alpha & g_b \left(1 + \xi \sin \left(\frac{2\pi t}{365} \right) \right) - \mu_b \end{bmatrix} \begin{bmatrix} I \\ B \end{bmatrix} + \begin{bmatrix} R_1 \\ -g_b \frac{B^2}{k_t} \left(1 + \xi \sin \left(\frac{2\pi t}{365} \right) \right) \end{bmatrix}, \\ &\leq \begin{bmatrix} \frac{\Lambda}{\mu_h} \beta_{t_1} - q & \frac{\Lambda \beta_{t_2}}{\mu_h k_t} \left(1 + \theta \sin \left(\frac{2\pi t}{365} \right) \right) \\ \alpha & g_b \left(1 + \xi \sin \left(\frac{2\pi t}{365} \right) \right) - \mu_b \end{bmatrix} \begin{bmatrix} I \\ B \end{bmatrix}. \end{aligned}$$

It follows from Theorem (6) that $\lim_{t \rightarrow \infty} [I, B]^T \leq \lim_{t \rightarrow \infty} [\tilde{I}_t, \tilde{B}_t]^T = [0, 0]^T$, thus $\lim_{t \rightarrow \infty} [I, B]^T = [0, 0]^T$.

Theorem 7. *If $\mathcal{R}_0 < 1$, the following statements are valid for model (1):*

- a) $\lim_{t \rightarrow \infty} R = 0$.
- b) $\lim_{t \rightarrow \infty} S = \Lambda/\mu_h$.

Proof.

- a) We want to show that for any $v > 0$, there exists $\gamma \in \mathbb{R}^+$, such that if $t > \gamma$, then $R < v$.

Assume $\mathcal{R}_0 < 1$. Since $\lim_{t \rightarrow \infty} I = 0$, it follows that for any $v > 0$, there exists $\gamma_1 \in \mathbb{R}^+$, such that

$$(15) \quad t > \gamma_1 \implies I(t) < \frac{(\mu_h + \rho)}{\varepsilon} v.$$

Choose $\gamma \geq \gamma_1$. Since $\dot{R} = \varepsilon I - (\mu_h + \rho)R$, it follows from (15) that $t > \gamma$ implies $\dot{R} < (\mu_h + \rho)(v - R)$. The solution to the differential inequality, $\dot{R} < (\mu_h + \rho)(v - R)$, is $R < v - M \exp(-t(\mu_h + \rho))$ for some positive constant M . Indeed $R < v$.

- b) Since $N = S + I + R$, it follows from $\lim_{t \rightarrow \infty} R = 0$ and $\lim_{t \rightarrow \infty} I = 0$ that $\mathcal{R}_0 < 1$ implies $\lim_{t \rightarrow \infty} N = \lim_{t \rightarrow \infty} S = \Lambda/\mu_h$.

□

We thus have the following result.

Theorem 8. *The disease free equilibrium, \mathbf{x}_0 , of system (1) is globally asymptotically stable whenever $\mathcal{R}_0 < 1$.*

3. NUMERICAL RESULTS

In this section, simulation results are carried out through MATLAB. We hypothetically choose the following initial conditions and the parameter values in Table (1). The initial conditions used were $S(0) = 99980$, $I(0) = 20$, $R(0) = 0$, $B(0) = 40000$.

Table (1) shows the parameters of the typhoid model. On the same table, we include a column that shows the most sensitive parameters in the model. The human birth rate, Λ , has the highest

sensitivity with sensitivity index equal to one. It is followed by the human natural death rate, μ_h , with a sensitivity index of -0.9901 .

Table 1. Parameter Estimation and Sensitivity Analysis

Parameter	Range	Point Value	Source
β_{t_1}	0 – 1	7.5×10^{-5}	Assumed
β_{t_2}	0 – 1	1.97×10^{-11}	[23, 25]
δ	0.001 – 1	0.06	[23]
ρ	0 – 1	1.3×10^{-3}	[27]
g_b	0 – 1	0.014	[25]
α	0 – 20	10	[25]
μ_b	0 – 1	0.0345	[25]
Λ	100 – 467	449.31	[5]
μ_h	0.019 – 0.021	0.02	[16]
ε	0 – 1	0.1	[2, 24]
κ_t	0 – 1	0.62	Assumed
k		0.2	Assumed
k_t		500000	Assumed

3.1. Sensitivity Analysis. We begin by considering the sensitivity analysis of the model parameters to the model output. The Latin Hypercube sampling method was used. This method produced a set of partial rank correlation coefficients (PRCC) between each of the model parameters and the state variable I . The simulation was carried out over 1000 runs. The human birth rate, Λ , is the most sensitive parameter relative to the infectious class, and it is positively correlated to the infectious class. The natural human death rate, μ_h , is the second most sensitive parameter relative to the infectious class, and it is negatively correlated to the infectious class.

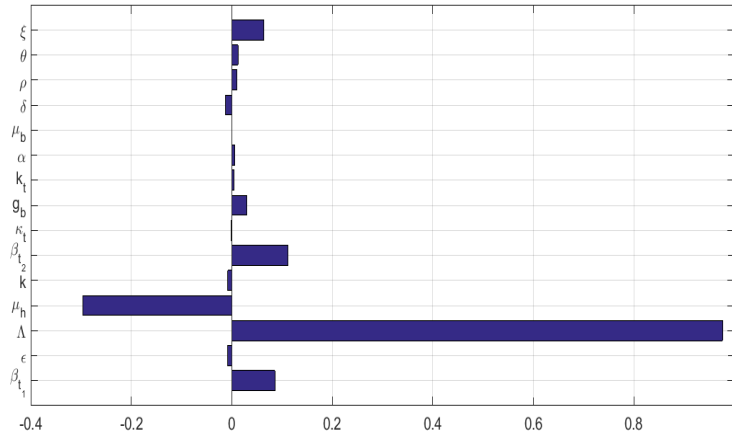


Figure 2. The partial rank correlation coefficients (PRCC). The correlation coefficients between the each of the parameters on Table 1 and the state variable I are shown. Parameters with negative PRCC values are negatively correlated to I , whilst those with positive PRCC values are positively correlated to I .

3.2. Plots of the reproduction numbers and the trajectories. The graph of the basic reproduction number, \mathcal{R}_0 , superimposed on the graph of the time average basic reproduction number, $[\mathcal{R}_0]$, is shown in Fig 3. The time average basic reproduction number was computed by setting the the direct transmission rate $\beta_{t_1} = 7.5 \times 10^{(-6)}$. Using the same direct transmission rate and the method outlined in [29], we numerically computed the basic reproduction number when $\xi = 0$. Since the seasonal period of the disease is 365 days, the rate of exponential decay in all expressions containing the period will be fast. This then means that iterations exceeding five in such terms will achieve minimal improvement in the accuracy. It is for this reason that we have set $M = 10$ and $n = 100$ as defined in [29].

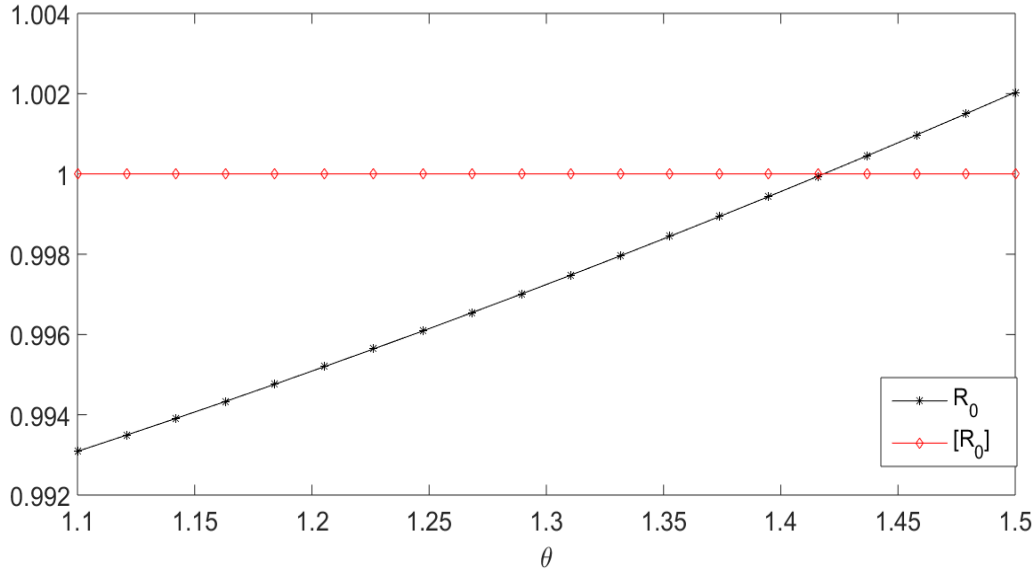


Figure 3. A comparison of the basic reproduction number, \mathcal{R}_0 , and the time average basic reproduction number $[\mathcal{R}_0]$ as a function of the seasonal parameter θ .

We consider the seasonal plots for our models (with and without) seasonality. The trajectories of all the state variables are shown in Figure 4. This figure shows the trajectories of the: (a), the susceptible class; (b), the infectious class; (c), the recovered class; and (d) the bacterial class. In each of the four figures in Figure 4, the trajectories of the seasonal model (1) are superimposed onto the trajectories of the non-seasonal model (2).

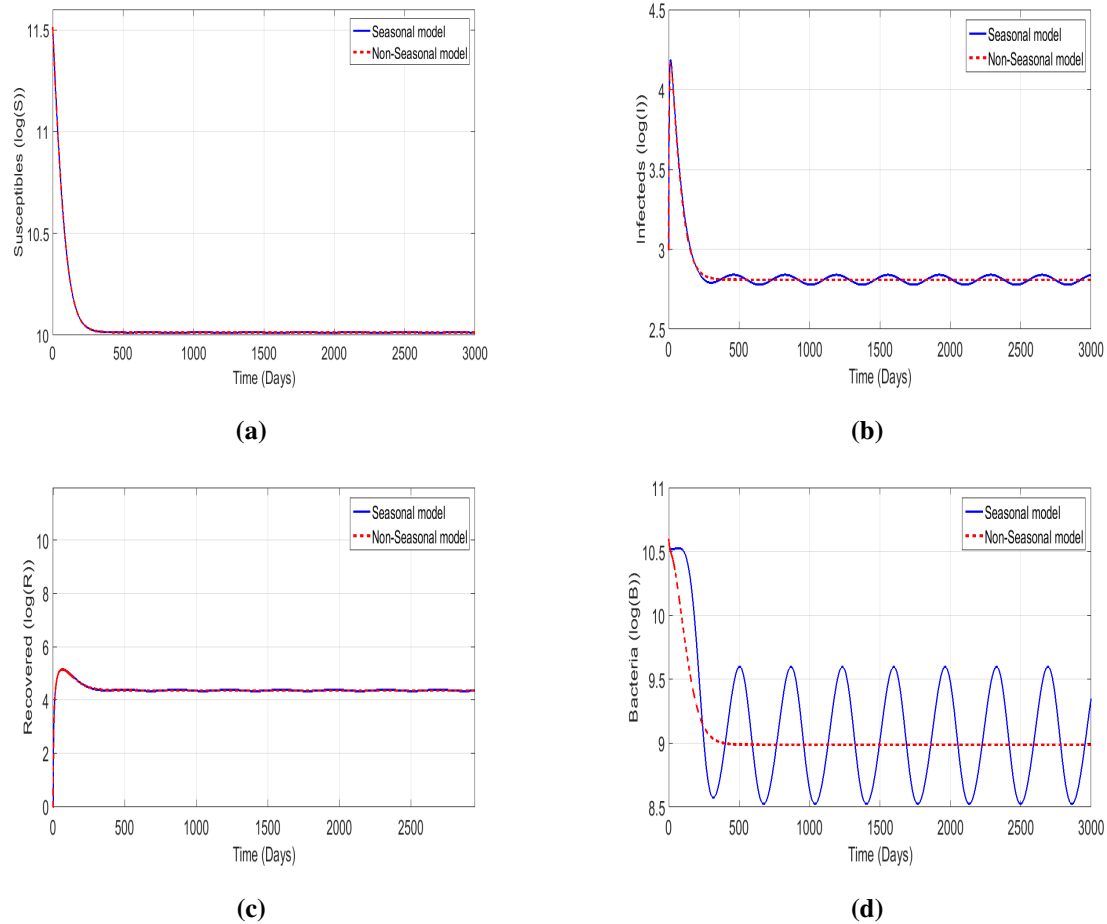
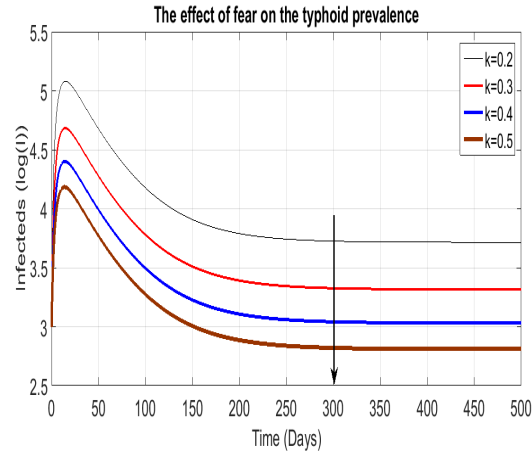
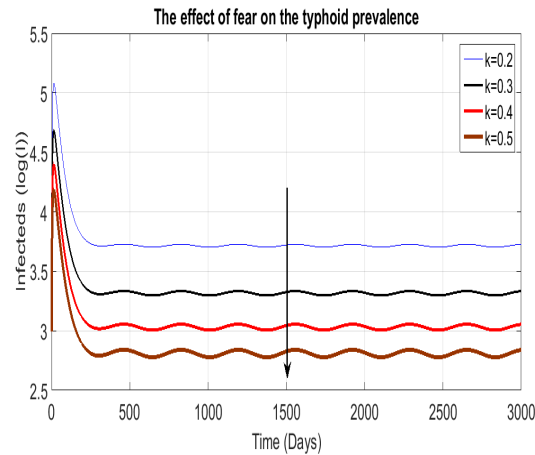


Figure 4. The trajectories of the models. The dotted lines depict the trajectories of the non-seasonal model (2), whilst the solid lines depict the trajectories of the seasonal model (1). The trajectories of the susceptibles, (a), the infecteds, (b), the recovered, (c), and the typhoid bacteria, (d) are shown.

3.3. Modelling the role of fear. We now consider the potential impact of fear on the model with and without seasonality. We use the logarithmic scale for clarity of presentation of results. The manner in which fear affects the prevalence of typhoid is shown in Figure 5. Figure 5(a) shows this effect on the non-seasonal model (2), whilst Figure 5(b) shows the same effect on the seasonal model (1). In both cases, the fear constant k is allowed to run through the set $\{0.2, 0.3, 0.4, 0.5\}$.



(a)



(b)

Figure 5. Typhoid prevalence as a function of fear. The fear constant, k , runs through $\{0.2, 0.3, 0.4, 0.5\}$. The effects of fear on the typhoid prevalence of the non-seasonal model (2) are shown in (a). The effects of fear on the typhoid prevalence of the seasonal model (1) are shown in (b).

4. DISCUSSION AND CONCLUSION

Seasonality is a common phenomenon in bacterial infections such as cholera and typhoid in which the diseases are more prevalent in summer than in winter. The spread of these diseases is further compounded by poor hygiene and maintenance of sewage disposal infrastructure. The mechanisms that drive seasonality in typhoid fever are mainly driven by rainfall patterns and poor sewage disposals system especially during summer. While some work has recently been done in [32]. The role of fear, which impacts the rate of infection was not considered. Fear

of infection has the propensity to reduce the infection rate and in this paper, our interest was on investigating how the seasonality dynamics of typhoid fever are impacted by fear. In this paper, we propose and analyze a model of typhoid fever that follows the work presented in [22] in the presence of fear. The model is motivated by the fact that in the presence of poor health infrastructure, behaviour changes become critical in the reducing the rate of typhoid fever infection in seasonally fluctuating environments. In addition, we are also motivated by scenarios in many countries in Sub-Saharan Africa, such as Zimbabwe, where typhoid fever remains a problem especially in Summer.

The seasonal fluctuations are modelled by the inclusion of a trigonometric function in the transmission rate driven by the bacterial population. The model is considered in cases where there is no seasonality and in the presence of seasonal fluctuations. In both cases, the basic reproduction numbers \mathcal{R}_0 and $[\mathcal{R}_0]$ are determined.

The stability of the steady states is carried out and we noted that the disease free equilibrium is globally stable when the basic reproduction number is less than unit. The existence of the endemic equilibrium is also discussed.

Numerical simulations are carried out following some hypothetical initial conditions and some chosen parameter values from the literature. Sensitivity analysis is also carried out using the Latin hyper cube sampling technique and the model is sensitive to the addition of susceptible individuals and the natural mortality rate of the human population.

It is important to note that the model presented in this paper has a number of limitations, as is the case with all mathematics models in which various assumptions are used in the construction of the models. The model is not validated by data. In the presence of data (which was not readily available in this case) the model would have been more robust, and in this case remains a theoretical model. This forms the basis of our future work. Despite this short coming, the model remains of great interest in the investigation of the role of human behaviour, such as fear in bacterial infections.

CONFLICT OF INTERESTS

The author(s) declare that there is no conflict of interests.

REFERENCES

- [1] GBD 2013 Mortality and Causes of Death Collaborators, Global, regional, and national age–sex specific all-cause and cause-specific mortality for 240 causes of death, 1990–2013: a systematic analysis for the Global Burden of Disease Study 2013, *Lancet*. 385 (2015), 117–171.
- [2] I.A. Adetunde, Mathematical Models for the Dynamics of Typhoid Fever in Kassena-Nankana District of Upper East Region of Ghana, *J. Mod. Math. Stat.* 2 (2008), 45–49.
- [3] B. Assan, F. Nyabadza, P. Landi, C. Hui, Modeling the transmission of Buruli ulcer in fluctuating environments, *Int. J. Biomath.* 10 (2017), 1750063-1–1750063-22.
- [4] C.P. Bhunu, W. Garira, Z. Mukandavire, Modeling HIV/AIDS and Tuberculosis Coinfection, *Bull. Math. Biol.* 71 (2009), 1745–1780.
- [5] K. Blayneh, Y. Cao, H-D Kwon, Optimal control of vector-borne diseases: Treatment and prevention, *Discrete Contin. Dyn. Syst.-B.* 11 (2009), 587.
- [6] C. Castillo-Chavez, Z. Feng, W. Huang, On the Computation of R_0 and its Role on Global Stability, in: C. Castillo-Chavez, S. Blower, P. van den Driessche, D. Kirschner, A.-A. Yakubu (Eds.), *Mathematical Approaches for Emerging and Reemerging Infectious Diseases: An Introduction*, Springer, New York, 2002: pp. 229–250.
- [7] N. Chitnis, D. Hardy, T. Smith, A Periodically-Forced Mathematical Model for the Seasonal Dynamics of Malaria in Mosquitoes, *Bull. Math. Biol.* 74 (2012), 1098–1124.
- [8] J. Crump, E. Mintz, Global Trends in Typhoid and Paratyphoid Fever, *Clinic. Infect. Dis.* 50 (2010), 241–246.
- [9] S. Del Valle, H. Hethcote, J.M Hyman, C. Castillo-Chavez, Effects of behavioral changes in a smallpox attack model, *Math. Biosci.* 195 (2005), 0–251.
- [10] P. van den Driessche, J. Watmough, Reproduction numbers and sub-threshold endemic equilibria for compartmental models of disease transmission, *Math. Biosci.* 180 (2002), 29–48.
- [11] J.M. Epstein, J. Parker, D. Cummings, R.A. Hammond, Coupled Contagion Dynamics of Fear and Disease: Mathematical and Computational Explorations, *PLoS ONE*. 3 (2008), e3955.
- [12] D. Greenhalgh, S. Rana, S. Samanta, T. Sardar, S. Bhattacharya, J. Chattopadhyay, Awareness programs control infectious disease – Multiple delay induced mathematical model, *Appl. Math. Comput.* 251 (2015), 539–563.
- [13] D.L. Heymann, *Control Of Communicable Diseases Manual*, American Public Health Association, New York, (2004).
- [14] M.T. Ho, A. Datta, S. Bhattacharyya, An elementary derivation of the Routh-Hurwitz criterion, *IEEE Trans. Automatic Control.* 3 (1998), 405–409.
- [15] J.A. Jacquez, C.P. Simon, *Qualitative Theory of Compartmental Systems*, *SIAM Rev.* 1 (1993), 43–79.

- [16] D.T. Jamison, R.G. Feachem, M.W. Makgoba, et al., eds. Disease and mortality in Sub-Saharan Africa. 2nd ed. The World Bank, Washington, 2006.
- [17] M.L. Juga, F. Nyabadza, Modelling the Ebola virus disease dynamics in the presence of interfered interventions, *Commun. Math. Biol. Neurosci.* 2020 (2020), 16.
- [18] M.J. Keeling, P. Rohani, *Modeling Infectious Diseases in Humans and Animals*, Princeton University Press, Princeton, 2007.
- [19] Y. Li, Z. Teng, S. Ruan, M-T. Li, X. Feng, A mathematical model for the seasonal transmission of schistosomiasis in the lake and marshland regions of China, *Math. Biosci. Eng.* 14 (2017), 1279-1299.
- [20] A. McLure, L. Furuya-Kanamori, A.C.A. Clements, M. Kirk, K. Glass, Seasonality and community interventions in a mathematical model of *Clostridium difficile* transmission, *J. Hosp. Infect.* 102 (2019), 157–164.
- [21] H.C. Moore, P. Jacoby, A.B. Hogan, C.C. Blyth, G.N. Mercer, Modelling the Seasonal Epidemics of Respiratory Syncytial Virus in Young Children, *PLoS ONE*. 9 (2014), e100422.
- [22] J. Mushanyu, F. Nyabadza, G. Muchatibaya, P. Mafuta, G. Nhawu, Assessing the potential impact of limited public health resources on the spread and control of typhoid, *J. Math. Biol.* 3 (2018), 647–670.
- [23] S. Mushayabasa, Impact of Vaccines on Controlling Typhoid Fever in Kassena-Nankana District of Upper East Region of Ghana: Insights from a Mathematical Model, *J. Mod. Math. Stat.* 5 (2011), 54-59.
- [24] S. Mushayabasa, Modeling the impact of optimal screening on typhoid dynamics, *Int. J. Dyn. Control.* 4 (2016), 330–338.
- [25] J.M. Mutua, F-B. Wang, N.K. Vaidya, Modeling malaria and typhoid fever co-infection dynamics, *Math. Biosci.* 264 (2015), 128–144.
- [26] N. Nyerere, L.S. Luboobi, S.C. Mpeshe, G.M. Shirima, A. Kloczkowski, Modeling the Impact of Seasonal Weather Variations on the Infectiology of Brucellosis, *Comput. Math. Meth. Med.* 2020 (2020), 8972063.
- [27] K.O. Okosun, O.D. Makinde, Modelling the impact of drug resistance in malaria transmission and its optimal control analysis, *Int. J. Phys. Sci.* 6 (2011), 6479–6487.
- [28] T.A. Phan, J.P. Tian, B. Wang, Dynamics of cholera epidemic models in fluctuating environments, *Stoch. Dyn.* 21 (2021), 2150011.
- [29] D. Posny, J. Wang, Computing the basic reproductive numbers for epidemiological models in nonhomogeneous environments, *Appl. Math. Comput.* 242 (2014), 473–490.
- [30] D. Posny, J. Wang, Modelling cholera in periodic environments, *J. Biol. Dyn.* 8 (2014), 1–19.
- [31] K. Prem, Y. Liu, T.W. Russell, et al. The effect of control strategies to reduce social mixing on outcomes of the COVID-19 epidemic in Wuhan, China: a modelling study, *Lancet Public Health.* 5 (2020), e261–e270.
- [32] N.J. Saad, V.D. Lynch, M. Antillón, et al. Seasonal dynamics of typhoid and paratyphoid fever, *Sci. Rep.* 8 (2018), 6870.

- [33] P.D. Shapiro, How close is too close?: The negative relationship between knowledge of HIV transmission routes and social distancing tendencies, *Soc. Sci. J.* 42 (2005), 629-637.
- [34] H.L. Smith, P. Waltman, *The Theory of the Chemostat: Dynamics of Microbial Competition*, Cambridge University Press, Cambridge, (1995).
- [35] G-Q. Sun, Z. Bai, Z-K. Zhang, T. Zhou, Z. Jin, Positive Periodic Solutions of an Epidemic Model with Seasonality, *Sci. World J.* 2013 (2013), 470646.
- [36] G. Teschl, *Ordinary Differential Equations and Dynamical Systems. Graduate Studies in Mathematics*, vol. 140. American Mathematical Society, Providence, 2012.
- [37] G.T. Tilahun, O.D. Makinde, D. Malonza, Co-dynamics of Pneumonia and Typhoid fever diseases with cost effective optimal control analysis, *Appl. Math. Comput.* 316 (2018), 438–459.
- [38] B. Traoré, B. Sangaré, S. Traoré, A Mathematical Model of Malaria Transmission with Structured Vector Population and Seasonality, *Journal of Applied Mathematics* 2017 (2017), 6754097.
- [39] A.C. Tsai, D.R. Bangsberg, S.M. Kegeles, et al. Internalized Stigma, Social Distance, and Disclosure of HIV Seropositivity in Rural Uganda, *Ann. Behav. Med.* 46 (2013), 285–294.
- [40] W. Wang, X-Q. Zhao, Threshold Dynamics for Compartmental Epidemic Models in Periodic Environments, *J. Dyn. Differ. Equ.* 20 (2008), 699–717.
- [41] X. Wang, D. Gao, J. Wang, Influence of human behavior on cholera dynamics, *Math. Biosci.* 267 (2015), 41–52.
- [42] X. Wang, L. Zanette, X. Zou, Modelling the fear effect in predator–prey interactions, *J. Math. Biol.* 73 (2016), 1179–1204.
- [43] World Health Organisation, Diarrhoeal Diseases, Typhoid Fever, https://web.archive.org/web/20111102190825/http://www.who.int/vaccine_research/diseases/diarrhoeal/en/index7.html, Accessed: 2021-01-11.
- [44] X. Yang, L. Chen, J. Chen, Permanence and positive periodic solution for the single-species nonautonomous delay diffusive models, *Computers Math. Appl.* 32 (1996), 109–116.
- [45] F. Zhang, X-Q. Zhao, A periodic epidemic model in a patchy environment, *J. Math. Anal. Appl.* 325 (2007), 496–516.